Published in
Solid State Sciences, vol. 11, pp. 1742–1746, 2009.

Electronic structure and conductivity of nanocomposite metal (Au,Ag,Cu,Mo)-containing amorphous carbon films

J. L. Endrino[1,2], D. Horwat[3], R. Gago[1], J. Andersson[2], Y.S. Liu[4], J. Guo[4], A. Anders[2]

[1] Instituto de Ciencias de Materiales de Madrid, Consejo Superior de Investigaciones Científicas, E-28049 Madrid, Spain
[2] Plasma Applications Group, Lawrence Berkeley National Laboratory, 1 Cyclotron Rd., Berkeley, CA 94720, USA
[3] Laboratoire de Science et Génie des Surfaces, Nancy-Université, CNRS, Parc de Saurupt CS 14234 F-54042 Nancy, France
[4] Advanced Light Source, Lawrence Berkeley National Laboratory, 1 Cyclotron Rd., Berkeley, CA 94720, USA

Manuscript May 14, 2008

Electronic structure and conductivity of nanocomposite metal(Au,Ag,Cu,Mo)-containing amorphous carbon films

J. L. Endrino[1,2], D. Horwat[3], R. Gago[1], J. Andersson[2], Y.S. Liu[4], J. Guo[4], A. Anders[2]

[1] Instituto de Ciencias de Materiales de Madrid, Consejo Superior de Investigaciones Científicas, E-28049 Madrid, Spain
[2] Plasma Applications Group, Lawrence Berkeley National Laboratory, 1 Cyclotron Rd., Berkeley, CA 94720, USA
[3] Laboratoire de Science et Génie des Surfaces, Nancy-Université, CNRS, Parc de Saurupt CS 14234 F-54042 Nancy, France
[4] Advanced Light Source, Lawrence Berkeley National Laboratory, 1 Cyclotron Rd., Berkeley, CA 94720, USA

Abstract.
In this work, we study the influence of the incorporation of different metals (Me = Au, Ag, Cu, Mo) on the electronic structure of amorphous carbon (a-C:Me) films. The films were produced at room temperature using a novel pulsed dual-cathode arc deposition technique. Compositional analysis was performed with secondary neutral mass spectroscopy whereas X-ray diffraction was used to identify the formation of metal nanoclusters in the carbon matrix. The metal content incorporated in the nanocomposite films induces a drastic increase in the conductivity, in parallel with a decrease in the band gap corrected from Urbach energy. The electronic structure as a function of the Me content has been monitored by x-ray absorption near edge structure (XANES) at the C K-edge. XANES showed that the C host matrix has a dominant graphitic character and that it is not affected significantly by the incorporation of metal impurities, except for the case of Mo, where the modifications in the lineshape spectra indicated the formation of a carbide phase. Subtle modifications of the spectral lineshape are discussed in terms of nanocomposite formation.

1. INTRODUCTION

Incorporation of metals inside a carbon host matrix is an interesting approach to tailor the properties of the carbon-based materials. This is of particular interest in the case of amorphous carbon (a-C) films due to their potential as coating material in mechanical, biomedical and electronic applications. In this study, a-C refers to a disordered non-hydrogenated mixture of sp^2 and sp^3 C atoms where the proportion of sp^3 sites is below 30%, in contrast to the "diamond-like" structure which usually refers to films with a dominant sp^3 character (>80%). High thermal and chemical stability and a strong corrosion resistance are among the common interesting properties of these films [1].

Recently, much attention has been paid to metal-containing a-C (a-C:Me) films due to their low cost and wide variety of properties [2-4]. The advantage of a-C:Me films as electronic materials is that their conductivity behavior can be varied from dielectric to metallic by slight changes in their composition [5]. Also, incorporation of metals may induce other interesting properties such as reduced film stress [6] or improved tribological properties [7].

Previous studies on metal-containing carbon films has been mainly focused on hydrogenated a-C films deposited using hybrid physical (PVD) and chemical (CVD) vapor deposition techniques involving either magnetron sputtering or cathodic arc deposition of the metal phase in a reactive hydrocarbon gas environment [3, 8]. However, less attention has been given to the non-hydrogenated counterpart. The production of hydrogen-free a-C:Me

films have been addressed by PVD techniques such as pulsed laser deposition from mixed metal-graphite targets [4], by the use of two separate cathodic arc sources in synchronous mode [9] and, most recently, by the use of a pulsed dual-cathode arc deposition (PDC-FCVA) source containing independent graphite and metal cathodes [2]. The PDC-FCVA system in combination with a "species selective bias" was used that allows the application of bias to the substrate only when the carbon plasma was present. In this way, undesirable resputtering of the deposited film by the impinging of heavy and energetic metal ions was reduced [10]. It should be noted that the ions arriving at the substrate from the arc source do not carry only kinetic energy but potential energy as well, which can affect the properties of the growing structure and the bonding between the metal and carbon atoms.

Here, we present a comparative study of different metal (Au,Ag,Cu,Mo) incorporation in a-C by PDC-FCVA. The modification of the film properties and electronic structure of the films is addressed where, at the same time, the interaction between C and different metal atoms can provide additional information of the growth mechanisms in PDC-FCVA.

2. EXPERIMENTAL

2.1 Sample preparation

a-C/Me(Au,Ag,Mo,Cu) films were prepared on glass (microscope slides) and Si (100) substrates by PDCAD. The deposition system consisted of a dual-cathode "triggerless" mini-gun designed to operate in pulsed mode [11]. For a-C:Me deposition, the source was loaded with carbon and transition metal (Au, Ag, Mo, and Cu) cathodes. Pulsed arc discharges on individual cathodes were triggered by a computer control system. The pulses used in the production of carbon plasma were 100 A and had a duration of 5 ms, while the metal plasma was made using pulses 1 ms long and a current of 700 A. The plasma stream produced by the source is injected into a 90-degree filter to remove most of the macroparticles which were formed during the cathodic arc process. After exiting the filter, the plasma expanded through a homogenizer device composed of concentric magnets and allowed to have homogeneous thickness and composition in the substrates over an area of 78.5 cm^2. During the deposition of C active pulses, the substrates were biased with 1 kV pulses that were 2 μs long, and there was an off time of 14 μs while, the substrate was kept at ground potential during the deposition of the metal plasma (hence "species selective bias"). During the deposition, the substrate holder was rotated at a speed of 2 rpm. The residual gas pressure was typically in the 10^{-4} Pa range.

2.2. Sample characterisation

The metal (Au,Ag,Cu,Mo) contents in the films were measured by secondary neutral mass spectrometry (SNMS) with an 8 keV Ar^+ primary beam. The apparatus is a SimsLab-VG. The typical currents on the samples were in the range 300-500 nA and the sputtered atoms were post-ionised by the electrons emitted from a filament for the mass spectrometry analysis. The quantification procedure consisted in calibrations from the measurements of Au-Ti, Ag-Ti, Cu-Ti, Mo-Ti and Ti-C sputtered reference films and in the integration of the SNMS profiles obtained for the a-C:Me films.

The electrical conductivity was measured by the four point probe method on the films deposited on glass substrates via a Keithley 2700 multimeter and a Keithley 237 high-voltage source. The optical transmission measurements were performed on the same samples with a UV-visible-NIR Carry 5000 Varian Spectrophotometer for wavelengths ranging from 200 to 1500 nm. The optical direct band-gap energy, E_g, of the films was obtained in the $\alpha h\nu^{1/2}= f(h\nu)$ representation by the X-intercept of the extrapolated linear high energy part of the curve (known as the Tauc procedure) [12]. The Urbach energy, E_u, that quantifies the structural and

compositional disorder was deduced from the slope at hν = 1.5 eV of the ln α=f(hν) plot. The absorption coefficient, α, was determined using the expression λ=(1/d)ln(1/T), where d and T are the thickness and transmittance of the film, respectively.

The structural characteristics of the a-C:Me films were probed by grazing incidence X-ray diffraction (GIXRD) at an incident angle of 2° with respect to the substrate surface. The experiments were done with a Co-K_α source (wavelength of 0.179 nm) using an INEL diffractometer.

X-ray absorption near edge structure (XANES) was studied at beamline 7.0 of the Advanced Light Source (ALS) at Lawrence Berkeley National Laboratory. The experiments were performed by measuring simultaneously the total electron and total fluorescence (TFY) yields. For energy calibration, the monochromator position was adjusted using the π* resonance peak at 285.5 eV for highly oriented pyrolytic graphite (HOPG). The calculation of the sp^2 content has been estimated from the relative intensity of the π* and σ* signals normalized to the value of an evaporated C film (e-C), which is composed of ~95% sp^2 hybrids.

3. RESULTS AND DISCUSSION

3.1. Nanocomposite formation and properties in a-C:Me films

Table I shows the metal content for all four a-C :Me combinations as a function of the main deposition parameter, i.e. the pulse ratio applied to the C and Me cathodes. The complexity of the deposition system is reflected in the non linearity of the incorporated metal content with respect to the C/Me pulse ratio. For example, it can be noted that while the maximum incorporation of Au atoms into the a-C:Au film reached only 4.5 at.%, Cu, Ag, and Mo-doped samples reached higher metal contents of 13.6, 17.6 and 29.6 at.%, respectively. This could be in part explained by the differences in the cathodic arc ion erosion rates, the ion transport properties of the curved plasma filter, as well as by differences in the energetic condensation of the metal plasmas as a function of cathode material, which can affect the relative atomic content of carbon in the sample due to carbon re-sputtering. The kinetic energy of condensation of incoming ions is given:

$$E_{kin}(Q, t) = E_{kin,0} + Q\, e\, V_{bias}(t) \quad (1)$$

where $E_{kin,0}$ is the "natural" kinetic energy of the incoming ions, Q is the average charge state, e is the elementary charge, and V_{bias} is the applied bias voltage at a particular time. Although in the bias off-time the samples are grounded, there is still a small sheath to the plasma potential so there is still substantial kinetic energy even in the absence of "bias", adding some kinetic energy on top of the kinetic energy from the arc plasma generation. According to Ref. [13], the "natural" kinetic energy (averaged over the energy distribution function) would range in the present case from 49 eV for Au to 149 eV for Mo, with Cu and Ag having intermediate $E_{kin,0}$ of 57.4 and 67.8 eV, respectively. In addition to "sputtering effects" at the surface, filters transport ions of different energy with different efficiency, and therefore the distribution function can be distorted. Further, the range of penetration of the deposited metal ions also increases with their kinetic energy and can affect the subplantation mechanism of the grown carbon film, collisions of metal ions and carbon atoms during deposition, the reactivity of the metal species and thus also the properties of the nanocomposite.

The GIXRD patterns for a-C:Me films with the two highest metal content are shown in Figure 1. The diffraction patterns of the films with the two lowest metal contents were x-ray amorphous for all metal dopants. This analysis shows that metal nanoclusters appear in all the Me containing films above a certain threshold of a few at. %, except for the Mo case. The

composition threshold could be as high as 14.8 at. % in the Cu case and as low as 1.5 at. % in the Ag case. Further, the nature of the metal atoms also influenced the size of the metal clusters. So while, the average measured crystallite size for a-C:Au and a-C:Cu films was about 4 nm and 7 nm, respectively, the crystallite size for a-C:Ag was between 8 and 15 nm.

As expected, the incorporation of metals in a-C:Me films is associated with an increase in the electrical conductivity, all the more pronounced as the metal content increases (Fig.2a). Even if the incorporation process resulted in dispersed metal contents, the conductivity of a-C:(Au,Ag,Mo) films seems to lay on the same "universal" curve. This is a typical conduction behavior for a conductive phase percolating in a resistive medium over the percolating threshold [14]. In the meantime, the a-C:Cu family exhibits a different evolution. Plotting E_g-E_u as a function of the metal content (Fig.2b) gives some insights for understanding this behavior. The different curves seem all to exhibit a common Y-intercept around 2.75 eV while E_g was found close to 3.5 eV and to be very slightly affected either by the nature or the amount of the metal element. It is worth noting that the increase of the metal content mainly enhances an Eu increase i.e. widens the penetration of the band tails into the band-gap. This effect is all the more marked as the reactivity of the metal towards carbon is limited, which could indicate the introduction of defects in the bandgap due to the metal implantation. One possible explanation for the electrical behavior of a-C:Cu samples is the existence of a given composition threshold below which copper segregation does not occur due to the formation of Cu-based compounds. Moreover, the poor crystallinity exhibited by a-C:Cu films (Fig. 1) in comparison to the one for a-C:Au and a-C:Ag films with a similar metal content could be due to the presence of Cu_2O nanoparticles formed during the deposition.

3.2 Electronic structure by X-ray absorption near edge structure (XANES)

XANES has been used to study the bonding structure around C atoms in the host matrix of the nanocomposite films. Figure 2 shows the XANES-TFY C K-edge spectra of all the a-C:Me films for the lowest and highest Me content. For the all the dopants, the spectra for the lowest Me contents show a dominant π^* resonance peak at 285.0 eV indicating a graphitic character (high participation of sp^2 hybrids). The position of the resonance peak, slightly shifted to lower energy values with respect to HOPG, is a direct signature of disorder due to the amorphous character of the coatings. A small contribution from C=O bonds is also observed in all samples from the weak peak at ~289 eV

The spectral comparison from the lowest and highest Me-containing films shows that the C K-edge is not significantly affected by Au, Ag and Cu incorporation. This result indicates that C does not react with these Me atoms and that the sp^2 content in the C phase is not modified (±5%) upon Me incorporation. This should be related with the separation of C and Me phases and the formation of a nanocomposite, as derived by the GIXRD data in Figure 1. On the contraty, the formation of C-Mo bonds in a-C:Mo films is revealed by the filling of states in the 286-289 eV region, which is already observed for the lowest Mo content. Also, a broadening of the π^* states is observed for a-C:Au films, which is more remarkable for the highest content and could be related to additional structural disorder in the a-C phase due to the impingment and/or incorporation of such heavy atoms. It is also worth noting that, in the case of the highest Au,Cu-containing samples there is an intensity decrease for σ^* states above 295 eV. Since these films showed poorer adhesion to the substrate, this spectral distortion could be explained by stress increase within the film structure due to metal inclusions and/or nanocomposite formation [14].

For comparison of the incorporation of different metals in the C host matrix, Figure 4 shows the normalized XANES-TFY spectra for the a-C:(Ag,Cu,Mo) and a-C:Au samples with Me contents of ~15 and ~5 at. %, respectively. The spectra are plotted together with the spectrum from the reference e-C film (~95% sp^2 hybrids). The intensity of the π^* region with respect to e-C indicates that the sp^2/sp^3 ratio in the C matrix is around 80% for a-C:Cu and

75% for a-C:Ag. The promotion of sp3 sites with respect to e-C should be related to the higher energy of the impinging C atoms in the PDCAD system. In the case of a-C:Au, the intensity of the □* states shows a higher sp^2 content (similar to that of the e-C film), which should be related to excesive damage induced by the impingining of Au ions during the film growth. The sp^2 quantification in the case of a-C:Mo is not feasible due to the formation of carbide bonds.

4. CONCLUSIONS:

In this work, the influence of metal (Au,Ag,Cu,Mo) incorporation in the conductivity and structural properties of a-C:Me films has been studied. The samples were obtained by PDCAD using a "species selective bias" configuration where the substrates are grounded during the deposition of the metal ions but biased when carbon ions are condensing. The strong variation in metal content seem to correlate with the "natural" kinetic energy of metal used. GIXRD analysis shows that nanocomposite films were formed above an incorporation threshold of a few at. %, except for a-C:Mo films where carbide formation takes place. The electrical conductivity of a-C:(Au,Ag,Mo) films followed the trend as a function of the metal content, with a different behavior for a-C:Cu samples. It is hypothesized the existence of a given composition threshold below which Cu segregation does not occur. XANES shows that the amorphous C host matrix has a dominant graphitic character and that Me-C bonds are formed only for Mo incorporation. Further, the C structure is not significantly affected for increasing Au, Ag and Cu incorporation, indicating the segregation of Me and C phases in agreement with GIXRD. Finally, the spectral lineshape for σ^* states above 295 eV is modified for the highest Cu and Au incorporation, which is correlated with a poorer adhesion to the substrate, i.e. increase of stress within the film.

ACKNOWLEDGEMENTS

The authors acknowledge helpful conversations with Prof. Jose M. Albella. Financial support from the Marie Curie Outgoing Fellowship Grant MOIF-CT-2005-02195 is also gratefully acknowledged as well as the Wenner-Gren Foundation. Work at Lawrence Berkeley National Laboratory was supported by the U.S. Department of Energy under Contract No. DE-AC02-05CH11231.

REFERENCES

[1] J. Robertson, Materials Science and Engineering: R: Reports 37 (2002) 129.
[2] J. L. Endrino, R. Escobar Galindo, H. S. Zhang, M. Allen, R. Gago, A. Espinosa and A. Anders, Surface and Coatings Technology 202 (2008) 3675.
[3] R. Hauert, Diamond and Related Materials 12 (2003) 583.
[4] R. J. Narayan, Diamond and Related Materials 14 (2005) 1319.
[5] S. Kumar and C. Godet, Solid State Communications 130 (2004) 331.
[6] B. K. Tay, Y. H. Cheng, X. Z. Ding, S. P. Lau, X. Shi, G. F. You and D. Sheeja, Diamond and Related Materials 10 (2001) 1082.
[7] A. A. Voevodin, M. S. Donley and J. S. Zabinski, Surface and Coatings Technology 92 (1997) 42.
[8] O. R. Monteiro, M. C. Salvadori, M. Cattani, V. Mammaana and I. G. Brown, Thin Solid Films 308-309 (1997) 215.
[9] O. R. Monteiro, M.-P. Delplancke-Ogletree and I. G. Brown, Thin Solid Films 342 (1999) 100.
[10] A. Anders, N. Pasaja and S. Sansongsiri, Review of Scientific Instruments 78 (2007) 063901.
[11] A. Anders, I. G. Brown, R. A. MacGill and M. R. Dickinson, J. Phys. D: Appl. Phys. 31 (1998) 584.
[12] J. Tauc, in "Optical Properties of Solids", edited by A. F. (North-Holland, Amsterdam, 1969).
[13] A. Anders and G. Y. Yushkov, Journal of Applied Physics 91 (2002) 4824.
[14] R. Gago, B. Abendroth, J. I. Cerda, I. Jimenez and W. Moller, Physical Review B (Condensed Matter and Materials Physics) 76 (2007) 174111.

Figure Captions:

Figure 1. Grazing incidence X-ray diffraction (GIXRD) patterns for the two highest at. % for Au, Ag, Mo, and Cu containing a-C films.

Figure 2. (a) Evolution of electronic conductivity of Au, Ag, Mo, and Cu containing a-C samples relative to metal content. The evolutions for Au, Ag and Mo a-C films lay on a common curve fitted thanks to the effective medium theory (EMT, see [16]) using $\sigma = \sigma_2 \left(\frac{f_v Me - f_p}{1 - f_p} \right)^t$ with t = 2 (3D composite system), a percolation threshold $f_p = 0$ and $\sigma_2 = 8.10^4$ S.cm^{-1}. The metal volume fraction f_vMe was approximated to half of the atomic fraction due to the molar volumes of a-C (~5 g.cm^{-3}) compared to those of Au, Ag and Mo (close to 10 g.cm^{-3}). While the EMT assimilates σ_2 to the metal conductivity, we found a difference of a factor 5.4, 7.9 and 2.4 with the theoretical conductivities of Au, Ag and Mo respectively. This difference contains the dispersion in the metal behaviours, the error in the estimation of f_vMe and eventually the degradation of conductivity due to Me-C bonds (b) Evolution of optical band-gap measurements as a function of metal content.

Figure 3. C K-edge XANES-TFY for various a-C:Me(Au,Ag,Mo,Cu) samples with the lowest (dotted line) and highest (solid line) metal content.

Figure 4. Normalized C K-edge XANES spectra for ~15 at. % Ag, Cu, and Mo containing a-C:Me films and ~5 at. % a-C:Au film, together with the reference spectrum from an e-C film (~95% sp^2 hybrids).

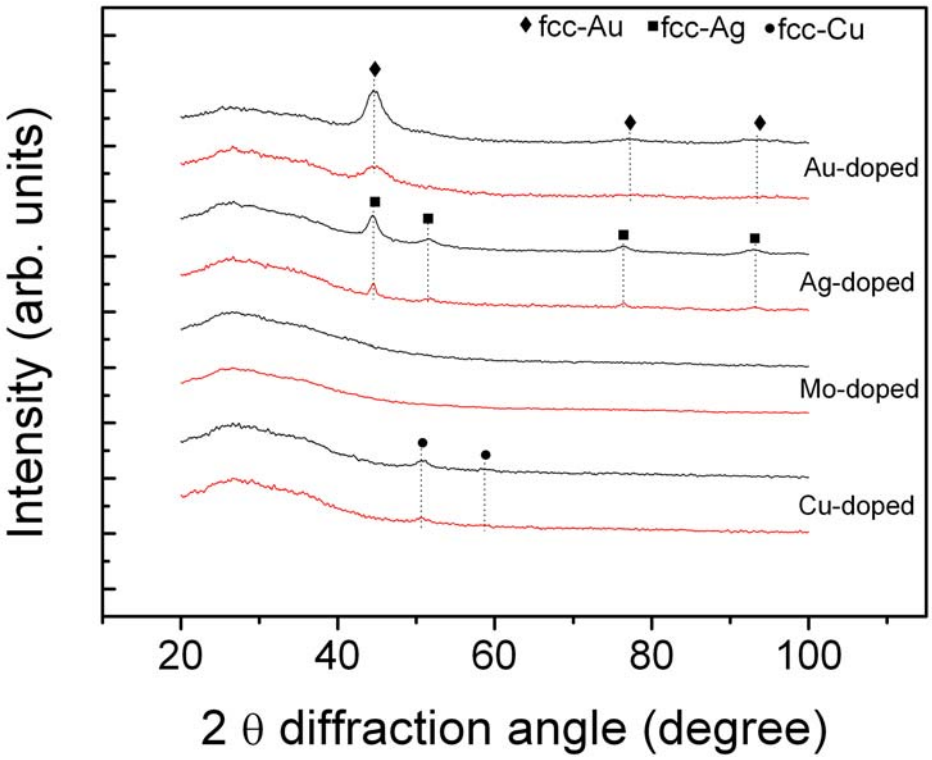
♦fcc-Au ■fcc-Ag •fcc-Cu
Au-doped
Ag-doped
Mo-doped
Cu-doped
Intensity (arb. units)
20
40
60
80
100
2 θ diffraction angle (degree)

Fig. 1

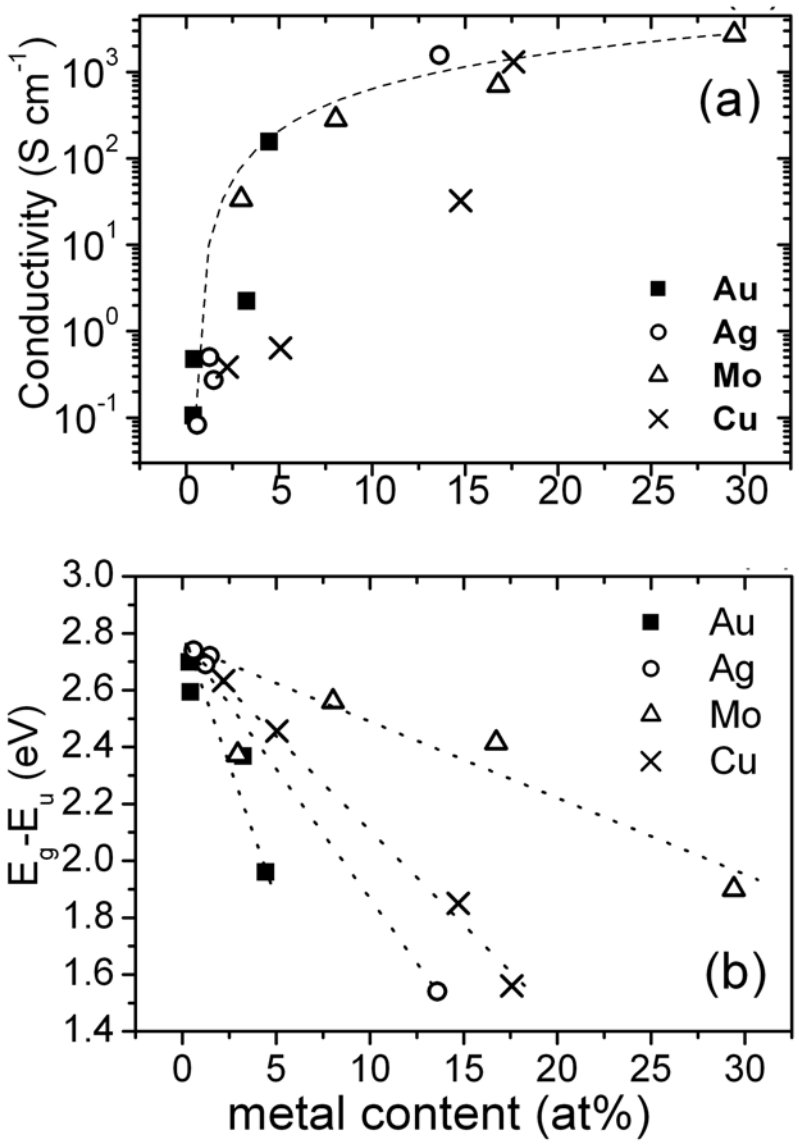
Conductivity (S cm^{-1})
10^{3}
10^{2}
10^{1}
10^{0}
10^{-1}
(a)
Au
Ag
Mo
Cu
0
5
10
15
20
25
30
E_g-E_u (eV)
3.0
2.8
2.6
2.4
2.2
2.0
1.8
1.6
1.4
Au
Ag
Mo
Cu
(b)
0
5
10
15
20
25
30
metal content (at%)

Fig. 2

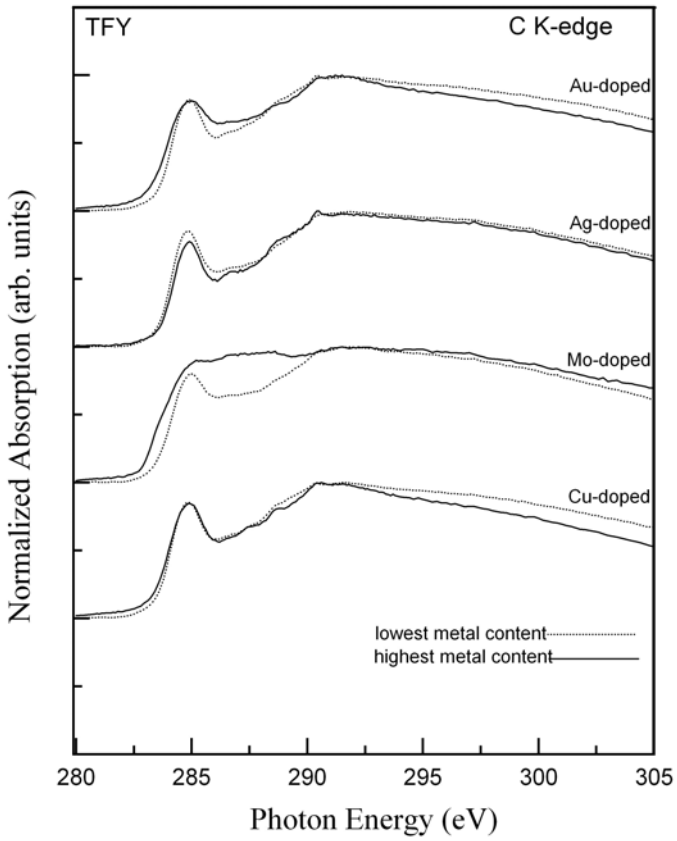
TFY
C K-edge
Au-doped
Ag-doped
Mo-doped
Cu-doped
lowest metal content
highest metal content
Normalized Absorption (arb. units)
280
285
290
295
300
305
Photon Energy (eV)

Fig.3

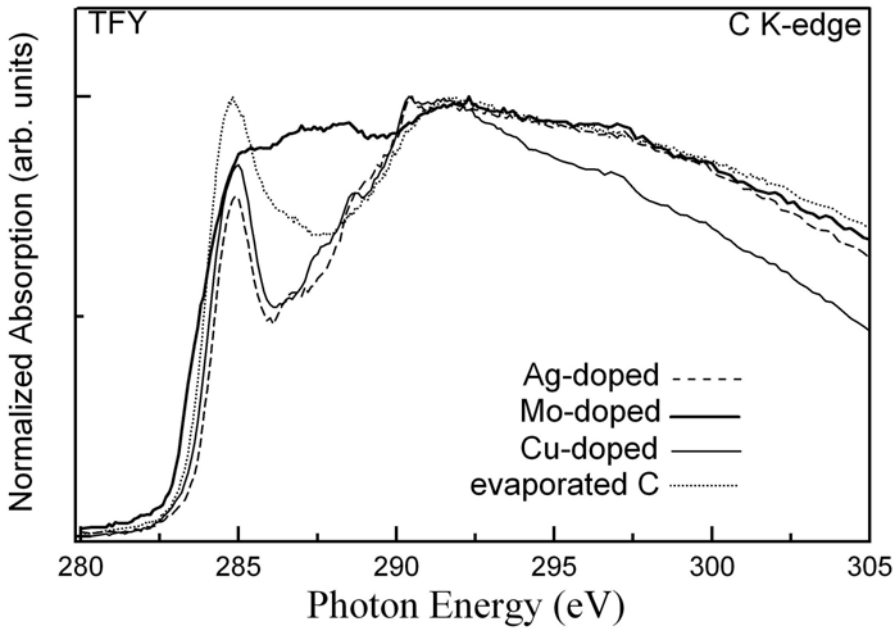
TFY
C K-edge
Normalized Absorption (arb. units)
Ag-doped
Mo-doped
Cu-doped
evaporated C
280
285
290
295
300
305
Photon Energy (eV)

Fig. 4

Table I. Average metal content in the a-C:Me films as determined by SNMS for each doping element..

C/Me deposition pulse ratio	***Au content in a-C:Au (at.%)***	***Ag content in a-C:Ag (at.%)***	***Mo content in a-C:Mo (at.%)***	***Cu content in a-C:Cu (at.%)***
24	0.3	0.6	3.0	2.2
12	0.5	1.2	8.1	5.1
6	3.3	1.5	16.8	14.8
3	4.5	13.6	29.6	17.6